Contents lists available at ScienceDirect

Arabian Journal of Chemistry

journal homepage: www.ksu.edu.sa

Therapeutic effect of total flavonoids of *Sargentodoxa cuneata* on ulcerative colitis in mice by correcting gut dysbiosis

Feng Xu [a,*], Piao Yu [a], Hongmei Wu [a], Xiangpei Wang [b], Mei Liu [a], Hongyun Liu [a], Qian Zeng [a], Dengli Wu [a]

[a] Guizhou University of Traditional Chinese Medicine, Department of Pharmacy, Guiyang, China
[b] Guizhou Minzu University, School of Chinese Ethnic Medicine, Guiyang, China

ARTICLE INFO

Keywords:
Total flavonoids of *Sargentodoxa cuneata*
Ulcerative colitis
Ulcerative colitis-related liver injury
Gut microbiota
Short-chain fatty acids
Organic acids

ABSTRACT

Sargentodoxa cuneata is a traditional Chinese herb commonly used for the treatment of ulcerative colitis (UC) in clinical practice. However, the effects of total flavonoids of *Sargentodoxa cuneata* (TFSc) remain unclear. In this study, we explored the effects and mechanisms of action of TFSc in mice with dextran sulfate sodium-induced UC. The TFSc components were identified using liquid chromatography-tandem mass spectrometry. Mice with UC were orally administered TFSc to evaluate its effects on colon and liver damage. Changes in gut microbiota were analyzed using 16S rRNA gene sequencing. Moreover, the levels of short-chain fatty acids (SCFAs) and few organic acids in the intestinal contents were measured. Furthermore, the correlation amongst gut flora, SCFAs, and organic acids was studied. A total of 304 compounds were identified. TFSc alleviated the symptoms of UC in mice, inhibited weight loss, reduced the disease activity index, and improved colon shortening along with cardiac and hepatic indices. Furthermore, TFSc mitigated pathological changes in the colon and liver, and reduced the TNF-α levels in colon tissues of mice with UC. TFSc also modulated intestinal flora disorders, increased the levels of four SCFAs (isocaproic acid, 3-hydroxyisovaleric acid, isobutyric acid, and ethylmethylacetic acid), and decreased the levels of two organic acids (malonic acid and succinic acid). The differential regulation of SCFAs and organic acids by TFSc was strongly associated with specific gut flora. TFSc showed potential for improving colon and liver injury in mice with UC by regulating the intestinal flora and associated metabolites (SCFAs and organic acids). These findings provide new evidence for developing TFSc as a drug for treating UC and UC-related liver injuries.

1. Introduction

Ulcerative colitis (UC) is a refractory diseases, as classified by the World Health Organization (Le Berre et al., 2023). In China, UC is one of the most common diseases of the digestive system, and is characterized by easy carcinogenesis and recurrent episodes (Cleveland et al., 2022). The morbidity and mortality rates of colorectal cancer caused by UC are extremely high, making it a serious threat to people's live and health (Le Berre et al., 2023). Clinical treatment of UC can only alleviate, but not cure the disease. The main therapeutic drugs for the inflammation of intestinal tract in the active stage of UC include aminosalicylic acid preparations, glucocorticosteroids, immunosuppressants, and biologics; however, there are shortcomings, such as poor therapeutic efficacy, more adverse reactions, and ease of recurrent after discontinuation of the drugs (Chen et al., 2022). Clinical findings on Chinese medicine for UC have shown that it has comprehensive efficacy in controlling intestinal inflammation, reducing complications, preventing disease recurrence after medication discontinuation, and improving patients' quality of life and prognosis (Liu et al., 2022).

According to Miao medicine, "poison is the source of all diseases" and "poison" staying in the gastrointestinal tract for a long time will affect the intestinal function and lead to organic lesions, such as inflammation, erosion, and ulcers. *Sargentodoxa cuneata* [the vine stem of *Sargentodoxa cuneata* (Oliv.) Rehd. et Wils.] belonging to the family Moutonaceae, also known as Da Xue Teng, has been used to treat gastrointestinal disorders. It reportedly detoxifies carbuncles, activates blood circulation, and relieves pain. Moreover, it also clears the heat, wind, and dampness poisons, and has a good therapeutic effect on UC

* Corresponding author at: College of Pharmacy Guizhou University of Traditional Chinese Medicine, Huaxi District, Guiyang City, Guizhou Province, Guiyang 550025, China.
E-mail address: xf333666999@sina.com (F. Xu).

https://doi.org/10.1016/j.arabjc.2023.105566
Received 5 October 2023; Accepted 13 December 2023
Available online 15 December 2023

(Zhang et al., 2021; Wang et al., 2023b). Furthermore, it has been elucidated that the ethyl acetate extract from decoction of *Sargentodoxa cuneata*, which is rich in total flavonoids, has a good therapeutic effect on UC (Yu et al., 2023b). Total flavonoids have antioxidant, anti-inflammatory, anticancer, and antiviral properties, and are one of the reported active components of traditional Chinese medicine against UC (Xue et al., 2023). Whether total flavonoids of *Sargentodoxa cuneata* (TFSc) is the active part of *Sargentodoxa cuneata* against UC remains unknow. Moreover, it would be interesting to know whether TFSc can also ameliorate the liver injury complicated by UC. However, the mechanism of action of TFSc in UC remains unclear and warrants further exploration.

In recent years, intestinal flora has been found to be involved in the pathogenesis and treatment of UC (Cheng et al., 2022). The microbial diversity in the intestinal tract of patients with UC is reduced in comparison to that of normal individuals. The abundance of bad bacteria increases and that of good bacteria decreases in the intestinal tract of patients with UC (Wang et al., 2023a). Intestinal flora and microbial metabolites are important for maintaining the intestinal health (Upadhyay et al., 2023). Therefore, changes in the composition of intestinal microbiota have a significant impact on the onset and treatment of UC. Regulation of disorders of the intestinal flora is an important way to treat diseases using herbal medicines (Wang et al., 2023a). After oral administration, the flavonoid components of Traditional Chinese Medicine either act directly on the intestinal flora or are absorbed into the bloodstream to exert a therapeutic effect (Cheng et al., 2023). Therefore, TFSc likely regulates gut dysbiosis caused by UC and ameliorates colonic and hepatic injuries in mice with UC.

In this study, the effects of TFSc on colon and liver injury in a mouse model of UC were assessed in the context of intestinal flora and its metabolites, such as short-chain fatty acids (SCFAs) and organic acids. The findings of our study will provide new ideas for elucidating the pharmacological mechanism of TFSc in the improvement of colon and liver injuries in UC, which would be conducive for the further development and utilization of TFSc.

2. Materials and methods

2.1. Chemicals and reagents

The 36–50 kDa dextran sulfate sodium (DSS) was obtained from MP Biomedical (Illkirch, France). Reagents (methanol and acetonitrile) used for chromatography were provided by Thermo-Fisher Scientific (Fair-Lawn, NJ, USA). Formic acid and standards of SCFAs and organic acids (≥99.9 % purity) were purchased from Sigma-Aldrich (St. Louis, MO, USA).

2.2. Preparation and composition of TFSc

The herbs used in this study were identified by Prof. Wang Xiangpei of the Guizhou Minzu University. An aqueous extract of *Sargentodoxa cuneata* was obtained by decocting with water, followed by filtration and concentration (Yu et al., 2023b). Briefly, the *Sargentodoxa cuneata* herb was weighted, and water was added to submerge the herbs 2–3 cm, soaked for 15 min, boiled over high heat, and then decocted over low heat for 15 min. The mixture was filtered and water was added water, followed by decoction. This procedure was repeated thrice. Finally, the filtrate was combined and concentrated using rotary evaporator. The extract was placed on a D101 macroporous resin column and eluted using different ethanol concentrations (5, 10, 20, 30, 40, 50, 70, and 95 %). After detection by sodium nitrite-aluminum nitrate colorimetric assay, 20 % and 40 % ethanol elution sites enriched in flavonoid components were combined, concentrated to no alcohol and dried to obtain TFSc.

An Agilent SB-C_{18} column (100 × 2.1 mm, 1.8 μm) was used to analyze the ingredients of TFSc at 40 °C. The mobile phase comprised 0.1 % formic acid aqueous solution (solvent A) and 0.1 % formic acid acetonitrile (solvent B) at 0.35 mL/min. The time program for gradient elution was as follows: 0–9 min, 5–95 % B, 9–10 min; 95 % B, 10–11.10 min; 95–5 % B, 11.10–14 min; 5 % B. Injection volume was 4 μL. A triple quadrupole-linear ion trap mass spectrometer was used to identify the composition of TFSc in positive and negative ion modes. Source temperature of electrospray ionization detector (ESI) was set at 500 °C, and ion spray voltage was set at 5500 V using positive ion mode and at −4500 V using negative ion mode. Instrument tuning and mass calibration were performed in triple quadrupole (QQQ) and LIT modes, respectively. A specific set of multiple-reaction monitoring (MRM) transitions was monitored for each period according to the metabolites eluted within that period. Based on the self-constructed local metabolic database of Biomarker Technologies (Beijing, China), the TFSc compounds were analyzed qualitatively and quantitatively using mass spectrometry.

2.3. Animals

Male C57BL/6 mice (18–22 g) were provided by SPF (Beijing) Biotechnology Co., Ltd (Beijing, China). All animals were kept in rooms maintained at 22–26 °C with a 12 h light, 12 h dark cycle. All animals were treated kindly and provided food and water ad libitum. Experiments were conducted in accordance with the requirements of the Animal Ethics Committee of Guizhou University of Traditional Chinese Medicine (N0. 20220046).

2.4. Mice with DSS-induced UC and drug administration

UC mouse models were constructed in accordance with the well-established methods (Fig. 2a). A total of 28 mice were randomly divided into control, UC, high-dose TFSc (39.02 mg/kg), and low-dose TFSc (19.51 mg/kg) groups. A 19.51 mg/kg dose of TFSc was equivalent to a human clinical dose of 0.25 g/kg of *Sargentodoxa cuneata*. Except for the animals in control group, which drank pure water, animals in other groups were giving water containing 2 % DSS for seven consecutive days, followed by pure water for another seven days. From days 1–14, the TFSc groups were administered TFSc at two different concentrations by intragastric gavage, whereas the control and UC groups were administered normal water.

2.5. Disease activity index (DAI) scoring and sampling

The animals were weighed every third days and on the last day. DAI was assessed on days 7, 10, and 13; and DAI scores included weight loss, stool consistency, and rectal bleeding scores. Weight loss was scored as 0–0 %, 1–1 %–5%, 2–5 %–10 %, 3–10 %–20 %, 4–>20 %, stool consistency as (0–negative; 1–malleable stool; 2–semi-sloppy stool; 3–loose stool; 4–severe loose stool); and rectal bleeding as (0–negative; 1–bloody stool visible to the naked eye (+); 2–++; 3–+++; 4–>+++). On day 14, animals of all the groups were sacrificed by cervical dislocation and the length of the colon tissue was measured. Moreover, the organ indices of heart, liver, spleen, lung, kidney, and thymus were also calculated. The colon and liver tissues were immobilized in 4 % paraformaldehyde solution, and the intestinal contents were collected for further experiments.

2.6. Histological evaluation

Colon and liver tissues were fixed with 4 % paraformaldehyde, processed, and stained using hematoxylin and eosin (HE) staining. Colon tissue damage index (TDI) scores comprised ulcer depth, degree of inflammatory cell infiltration, and depth of inflammatory cell infiltration scores. The following scores were allocated to the different damage parameters: depth of the ulcer (0, negative; 1, epithelium; 2, mucosal lamina propria; 3, mucosal muscularis propria), degree of inflammatory

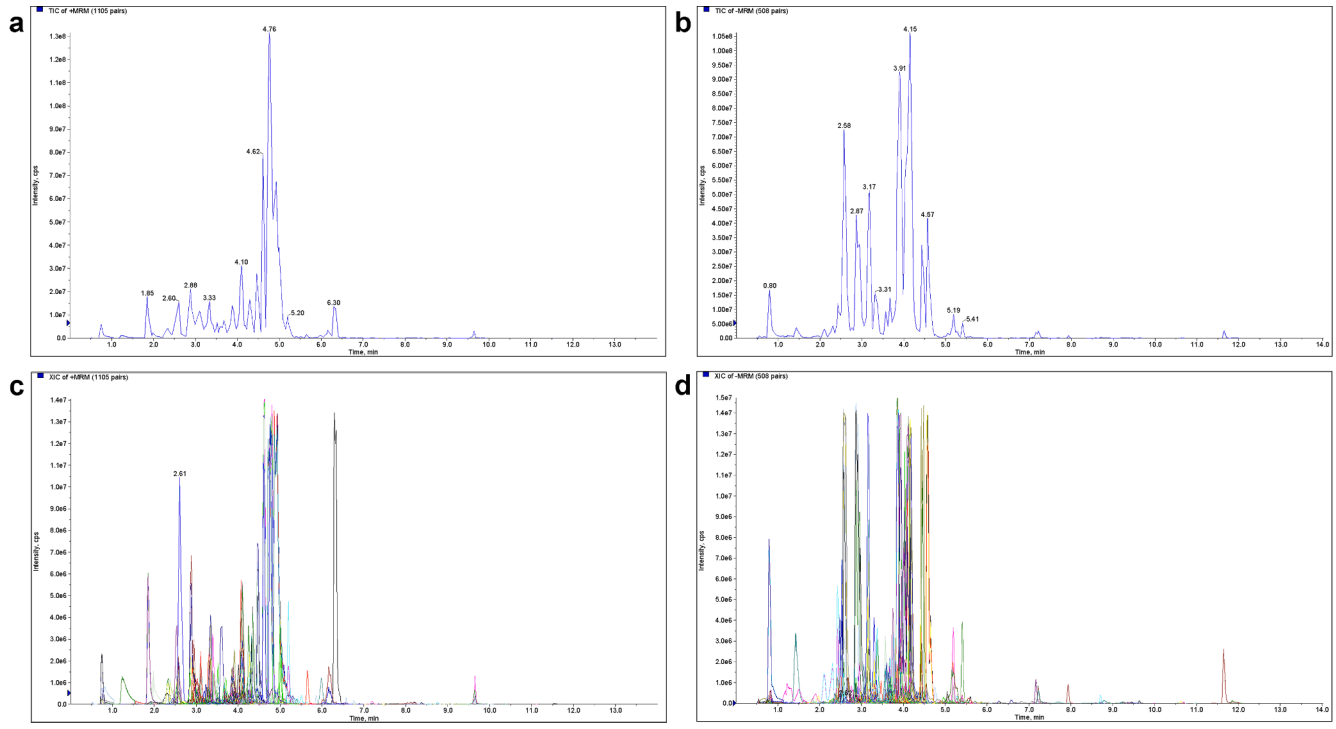

Fig. 1. Total ion chromatogram (TIC) and multiple-reaction monitoring (MRM) detection of multimodal maps of total flavonoids of *Sargentodoxa cuneata* (TFSc). (**a**) TIC in positive ion mode for TFSc sample. (**b**) TIC in negative ion mode for TFSc sample. (**c**) Positive ion mode for TFSc sample. (**d**) Negative ion mode for TFSc sample.

cell infiltration (0, negative; 1, mild; 2, moderate; 3, severe), and depth of inflammatory cell infiltration (0, negative; 1, mucosal layer; 2, mucosa and submucosa; 3, whole colon). Liver TDI scores consisted of cellular enlargement, cytoplasmic vacuolation, and narrowing of the hepatic sinusoids scores. The following scores were allocated to the different TDI parameters of liver: cellular enlargement (0, negative; 1, mild; 2, moderate; 3, severe), cytoplasmic vacuolation (0, negative; 1, mild; 2, moderate; 3, severe), narrowing of hepatic sinusoids (0, negative; 1, mild; 2, moderate; 3, severe).

2.7. Immunohistochemistry (IHC)

A wax block of colon tissue was taken and after deparaffinized using conventional methods and antigen was repaired with a citrate buffer solution. The sections were then incubated in 3 % hydrogen peroxide solution (hydrogen peroxide: purified water = 1:9) for 15 min at room temperature in dark to block endogenous peroxidase activity. The endogenous peroxidase activity was blocked by using 5 % goat serum for containment, and antibodies against tumor necrosis factor (TNF)-α (1:200, Affinity, Jiangsu, China) were added dropwise to the sections and incubated at 4 °C overnight. Next, secondary antibodies were added and incubated at 37℃ for 30 min, color developed using diaminobenzidine (DAB), restrained with Harris hematoxylin, and the sections were prepared for image acquisition. Hematoxylin-stained nuclei were blue, and positive staining with DAB appeared brownish-yellow.

2.8. 16S rRNA gene sequencing of the intestinal flora

The genomic DNA of each group was extracted from the fecal samples and prepared for PCR amplification of selected genes in specific regions of the primer using specific primers containing barcodes. Fluorescence was quantified using a Quant-iT PicoGreen dsDNA assay kit and a microplate reader as the fluorescence quantification instrument. (BioTek, FLx800, USA). Amplicon library size and quantity were assessed using Agilent Bioanalyzer (Agilent, United States), and sequencing was performed on Illumina platform. NovaSeq 6000 SP kit reagent was used for sequencing. The raw sequences were de-primed, quality-filtered, de-noised, spliced, and de-chimerised using the Divisive Amplicon Denoising Algorithm 2 (DADA2) in FASTQ format. Operational taxonomic unit (OTU) analysis was performed with >97 % similarity. The abundance information, α- and β-diversity, along with community structure and species composition of the samples were analyzed using multivariate analysis. Furthermore, differences in biologically relevant taxonomic biomarkers among the groups were analyzed using linear discriminant analysis effect size (LEfSe).

2.9. Measurement of SCFAs and organic acids in intestinal contents

The intestinal content sample was accurately weighed, water was added, and the sample was homogenized for 3 min using zirconia beads (B B24, Next Advance, Inc., NY, USA). The sample was then treated with methanol, and standard internal substances were added. After centrifugation, the supernatant was analyzed using Biomek 4000 workstation (California, USA). The samples were centrifuged and subjected to UPLC-MS/MS analysis. UPLC-Xevo TQ-S system (MA, USA) was used for analysis. A Waters ACQUITY UPLC BEH C_{18} column (2.1 × 100 mm, 1.7 μM) was used for separation at 40 °C. Gradient elution program [0–1 min, 12 % B; 1–2.8 min, 12–16.5 % B; 2.8–4.2 min, 16.5–24 % B; 4.2–5.6 min, 24–30 % B; 5.6–8.5 min, 30–100 % B; 8.5–10 min, 100 % B; 10–11 min, 100–1 % B; and 11–12 min, 1–12 % B (solvent A, 0.1 % formic acid; solvent B, acetonitrile)] was performed at 0.4 mL/min for the whole analytic process. Injection volume was 5 μL. The ESI ion source temperature was set at 150 ℃ using negative ion mode and the target ions were monitored.

2.10. Correlation analysis of intestinal microbiota with SCFAs and organic acids

SCFAs and organic acids have been found to be closely related to the

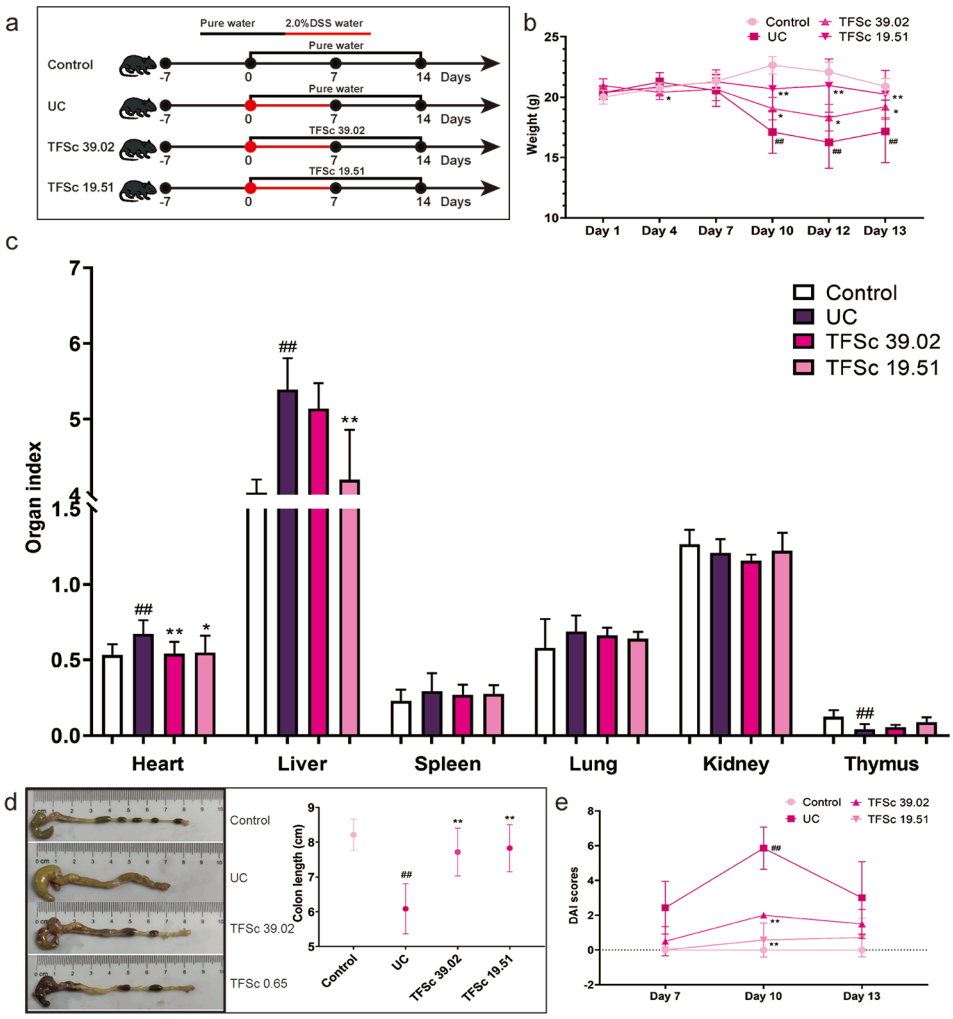

Fig. 2. Total flavonoids of *Sargentodoxa cuneata* (TFSc) improved the manifestations of mice with UC. (**a**) The process of this animal experiment. (**b**) Body weight changes. (**c**) Effects of TFSc on heart, liver, spleen, lung, kidney and thymus index scores. (**d**) The colon tissue and length. (**e**) DAI scores. Data are presented as mean ± SD (n = 7 per group). $^{\#}P < 0.05$ vs. the control group, $^{\#\#}P < 0.01$ vs. the control group, $^{*}P < 0.05$ vs. the UC group, $^{**}P < 0.01$ vs. the UC group.

intestinal flora and are important metabolites of intestinal flora (Lee et al., 2020). Spearman's correlation coefficients were calculated to identify bacteria-metabolite correlations.

2.11. Statistical analysis

For analysis of pharmacodynamic indicators, intestinal microbiota, SCFA, and organic acids, data were presented as mean ± standard deviation (SD). One-way ANOVA and least significant difference (LSD) test was used to analyze the results among the groups using SPSS 20.0 software (Chicago, Illinois, USA). The α-diversity differences between samples of different groups were analyzed using Wilcoxon's rank-order analysis. $P < 0.05$ represented a statistical difference, while $P < 0.01$ indicated more significant statistical difference.

3. Results

3.1. Analysis of the chemical constituents of TFSc using UPLC-MS

Broad-targeted metabolomic analysis identified 304 flavonoid components from TFSc. The major flavonoid components included flavanols, flavonols, flavones, dihydroflavonoids, dihydroflavonols, proanthocyanidins, chalcones, and isoflavones (Fig. 1, Table S1). The top 100 compounds in terms of metabolic abundance of the identified components are shown in Table 1. All the components were validated based on their accuracy and fragments. Components namely rutin, proanthocyanidin B2, epicatechin, catechin and quercetin have been reported previously (Lai, 2019, Zhang et al., 2021, Zhan et al., 2022).

3.2. TFSc ameliorated colon and liver injury in mice with DSS-induced UC

Mice in the UC group experienced dramatic weight loss during days 10–13 (Fig. 2b). TFSc (39.02 and 19.51 mg/kg) inhibited weight loss in mice (Fig. 2b). Unexpectedly, TFSc significantly decreased the DAI scores on day 3 (Fig. 2e). However, on day 13, TFSc only demonstrated a statistically insignificant reduction in DAI scores, suggesting that the animals were already in the recovery phase of UC. DSS significantly shortened the colon length compared to that in the control animals ($P < 0.01$) (Fig. 2d). TFSc (39.02 and 19.51 mg/kg) improved the colon length. To preliminarily examine the effects of TFSc on the major organs of mice with UC, we measured the organ indices in each group of mice. TFSc (39.02 and 19.51 mg/kg) decreased the heart index of mice with UC, and 19.51 mg/kg TFSc also significantly decreased the liver index. TFSc showed some improvement in the immune organs (spleen and thymus), but the difference was not statistically significant. Moreover, improvements were also seen in the lung and kidney (Fig. 2c).

HE staining revealed that the mucosal, submucosal, muscular, and outer membranes of the colon were disrupted and infiltrated with inflammatory cells in mice with UC (Fig. 3). TFSc (39.02 and 19.51 mg/

Table 1
The top 100 compounds in terms of metabolic abundance of the identified components in total flavonoids of *Sargentodoxa cuneata* (TFSc) using UPLC-Q-TOF/MS.

name	metabolite abundance	Formula	Molecular weight (Da)	Ionization model	Q1 (Da)	Class II
Catechin-(7,8-bc)-4α-(3,4-dihydroxyphenyl)-dihydro-2-(3H)-one	49998364.67	$C_{24}H_{20}O_9$	452.1107	$[M-H]^-$	451.1045	Flavanols
Cinchonain Id	45048595.01	$C_{24}H_{20}O_9$	452.1107	$[M-H]^-$	451.1045	Flavanols
Cinchonain Ic	7806603.636	$C_{24}H_{20}O_9$	452.1107	$[M-H]^-$	451.1033	Flavanols
Quercetin	7187682.949	$C_{15}H_{10}O_7$	302.0427	$[M+H]^+$	303.0518	Flavonols
Isobavachalcone glucoside	4585041.257	$C_{26}H_{30}O_9$	486.189	$[M+H]^+$	487.1911	Chalcones
Chrysoeriol-7-O-glucoside	3034536.541	$C_{22}H_{22}O_{11}$	462.1162	$[M-H]^-$	461.1084	Flavones
Quercetin-3-O-neohesperidoside*	2799344.01	$C_{27}H_{30}O_{16}$	610.1534	$[M+H]^+$	611.1594	Flavonols
Aromadendrin-7-O-glucoside	2594921.849	$C_{21}H_{22}O_{11}$	450.1162	$[M-H]^-$	449.1081	Flavanonols
Epicatechin	2509557.779	$C_{15}H_{14}O_6$	290.079	$[M+H]^+$	291.0859	Flavanols
Quercetin-3-O-glucoside-7-O-rhamnoside*	2506390.498	$C_{27}H_{30}O_{16}$	610.1534	$[M+H]^+$	611.1594	Flavonols
Hesperetin-7-O-(6″-malonyl)glucoside	2447186.468	$C_{25}H_{26}O_{14}$	550.1323	$[M-H]^-$	549.1247	Flavanones
Rutin*	2309914.321	$C_{27}H_{30}O_{16}$	610.1534	$[M+H]^+$	611.1591	Flavonols
Diosmetin-7-O-galactoside	1835744.129	$C_{22}H_{22}O_{11}$	462.1162	$[M+H]^+$	463.1232	Flavones
Homoplantaginin	1805320.246	$C_{22}H_{22}O_{11}$	462.1162	$[M+H]^+$	463.1232	Flavones
Quercetin-5-O-β-D-glucoside*	1748991.25	$C_{21}H_{20}O_{12}$	464.0955	$[M+H]^+$	465.104	Flavonols
Luteolin-8-C-arabinoside	1657264.21	$C_{20}H_{18}O_{10}$	418.09	$[M+H]^+$	419.0871	Flavones
6-C-MethylKaempferol-3-glucoside	1541284.5	$C_{22}H_{22}O_{11}$	462.1162	$[M+H]^+$	463.1232	Flavones
Naringenin-7-O-Rutinoside-4′-O-glucoside	1466638.281	$C_{33}H_{42}O_{19}$	742.232	$[M-H]^-$	741.231	Flavanones
Isohyperoside*	1,439,398	$C_{21}H_{20}O_{12}$	464.0955	$[M+H]^+$	465.102	Flavonols
6-C-Glucosyl-2-Hydroxynaringenin	1404154.322	$C_{21}H_{22}O_{11}$	450.1162	$[M-H]^-$	449.1094	Flavanones
Hesperetin-5-O-glucoside	1377354.268	$C_{22}H_{24}O_{11}$	464.1319	$[M-H]^-$	463.1241	Flavanones
Luteolin-3′-O-glucoside*	1321991.5	$C_{21}H_{20}O_{11}$	448.1006	$[M+H]^+$	449.1017	Flavones
Quercetin-3-O-robinobioside	1237069.255	$C_{27}H_{30}O_{16}$	610.1534	$[M-H]^-$	609.149	Flavonols
Hyperin	1170914.132	$C_{21}H_{20}O_{12}$	464.0955	$[M-H]^-$	463.0876	Flavonols
Luteolin-4′-O-glucoside*	1109268.5	$C_{21}H_{20}O_{11}$	448.1006	$[M+H]^+$	449.0985	Flavones
Quercetin-7-O-glucoside*	1087301.026	$C_{21}H_{20}O_{12}$	464.0955	$[M-H]^-$	463.0876	Flavonols
Spiraeoside*	1051313.626	$C_{21}H_{20}O_{12}$	464.0955	$[M-H]^-$	463.0876	Flavonols
Eriodictyol-8-C-glucoside	997562.653	$C_{21}H_{22}O_{11}$	450.1162	$[M-H]^-$	449.1086	Flavanones
Cynaroside*	732526.25	$C_{21}H_{20}O_{11}$	448.1006	$[M+H]^+$	449.1071	Flavones
Isoquercitrin	705213.947	$C_{21}H_{20}O_{12}$	464.0955	$[M-H]^-$	463.0876	Flavonols
Cinchonain Ia	629669.302	$C_{24}H_{20}O_9$	452.1107	$[M+H]^+$	453.1189	Flavanols
Chrysoeriol-7-O-(2″-O-glucuronyl)glucoside	596928.25	$C_{28}H_{30}O_{17}$	638.1483	$[M+H]^+$	639.1562	Flavones
Chrysoeriol-5-O-glucoside	549181.737	$C_{22}H_{22}O_{11}$	462.1162	$[M-H]^-$	461.1086	Flavones
Morin	548929.585	$C_{15}H_{10}O_7$	302.0427	$[M-H]^-$	301.0347	Flavonols
Quercetin-3,7-Di-O-glucoside	504937.626	$C_{27}H_{30}O_{17}$	626.1483	$[M+H]^+$	627.144	Flavonols
6-Hydroxykaempferol-3,6-O-Diglucoside	496,929	$C_{27}H_{30}O_{17}$	626.1483	$[M+H]^+$	627.1557	Flavonols
Procyanidin B1	489811.637	$C_{30}H_{26}O_{12}$	578.1424	$[M-H]^-$	577.1389	Proanthocyanidins
Trifolin	470898.384	$C_{21}H_{20}O_{11}$	448.1006	$[M-H]^-$	447.0955	Flavonols
6-Hydroxykaempferol-7,6-O-Diglucoside	461,937	$C_{27}H_{30}O_{17}$	626.1483	$[M+H]^+$	627.1562	Flavonols
Nepetin-7-O-alloside*	455715.75	$C_{22}H_{22}O_{12}$	478.1111	$[M+H]^+$	479.1202	Flavones
Neodiosmin*	440,225	$C_{28}H_{32}O_{15}$	608.1741	$[M+H]^+$	609.1825	Flavones
Nepitrin*	409857.5	$C_{22}H_{22}O_{12}$	478.1111	$[M+H]^+$	479.12	Flavones
4′-Methoxyflavone	403186.449	$C_{16}H_{12}O_3$	252.0786443	$[M-H]^-$	251.071	Flavones
6-C-Methylquercetin-3-O-rutinoside	397080.5	$C_{28}H_{32}O_{16}$	624.169	$[M+H]^+$	625.1765	Flavonols
Isorhamnetin-3-O-neohesperidoside	389677.5	$C_{28}H_{32}O_{16}$	624.169	$[M+H]^+$	625.1763	Flavonols
Sexangularetin-3-O-glucoside-7-O-rhamnoside	384112.5	$C_{28}H_{32}O_{16}$	624.169	$[M+H]^+$	625.1763	Flavonols
Sieboldin	344911.655	$C_{21}H_{24}O_{11}$	452.1319	$[M-H]^-$	451.1232	Chalcones
3,4,2′,4′,6′-Pentahydroxychalcone-4′-O-glucoside	326019.713	$C_{21}H_{22}O_{11}$	450.1162	$[M-H]^-$	449.1093	Chalcones
Diosmin*	307902.5	$C_{28}H_{32}O_{15}$	608.1741	$[M+H]^+$	609.1825	Flavones
8-Methoxykaempferol-7-O-rhamnoside	291909.008	$C_{22}H_{22}O_{11}$	462.1162	$[M-H]^-$	461.1095	Flavonols
Dihydromarein	276681.341	$C_{21}H_{24}O_{11}$	452.1319	$[M-H]^-$	451.1277	Chalcones
Calycosin-7-O-glucoside	263,752	$C_{22}H_{22}O_{10}$	446.1213	$[M+H]^+$	447.1285	Isoflavones
Tricetiflavan	254585.618	$C_{15}H_{14}O_6$	290.079	$[M-H]^-$	289.0738	Flavanols
Myricetin-3,7,3′-trimethyl ether	245411.196	$C_{18}H_{16}O_8$	360.0845	$[M-H]^-$	359.0774	Flavonols
6-Hydroxykaempferol-7-O-glucoside	245147.25	$C_{21}H_{20}O_{12}$	464.0955	$[M+H]^+$	465.1031	Flavonols
Vitexin-2″-O-galactoside	243922.5	$C_{27}H_{30}O_{15}$	594.1585	$[M+H]^+$	595.1678	Flavones
Isoorientin	240083.436	$C_{21}H_{20}O_{11}$	448.1006	$[M-H]^-$	447.0928	Flavones
5,7,3′-Trihydroxy-4,6,5′-trimethoxyxanthone	233613.128	$C_{17}H_{14}O_8$	346.0689	$[M-H]^-$	345.0608	Other Flavonoids
Kaempferol-3-O-(6″-Acetyl)glucosyl-(1 → 3)-Galactoside	215384.976	$C_{29}H_{32}O_{17}$	652.1639	$[M-H]^-$	651.1586	Flavonols
Prunin	210995.971	$C_{21}H_{22}O_{10}$	434.1213	$[M-H]^-$	433.1168	Flavanones
catechin-4-β-D-galactopyranoside*	199780.725	$C_{21}H_{24}O_{11}$	452.1319	$[M-H]^-$	451.125	Flavanols
Procyanidin B2	199226.75	$C_{30}H_{26}O_{12}$	578.1424	$[M+H]^+$	579.1507	Proanthocyanidins
3,3′-O-Dimethylellagic Acid	198507.964	$C_{16}H_{10}O_8$	330.0376	$[M+H]^+$	331.0442	Tannin
Epicatechin-3′-O-β-D-glucopyranoside*	186447.536	$C_{21}H_{24}O_{11}$	452.1319	$[M-H]^-$	451.1252	Flavanols
Procyanidin B5	185176.446	$C_{30}H_{26}O_{12}$	578.1424	$[M+H]^+$	579.1491	Proanthocyanidins
7-Benzyloxy-5-hydroxy-3′,4′-methylenedioxyflavonoid	183644.789	$C_{23}H_{16}O_6$	388.0947	$[M-H]^-$	387.1648	Flavones
Genistein-7-O-galactoside	182978.5	$C_{21}H_{20}O_{10}$	432.1056	$[M+H]^+$	433.1129	Isoflavones
Lonicerin*	165518.25	$C_{27}H_{30}O_{15}$	594.1585	$[M+H]^+$	595.1674	Flavones
Procyanidin B3	164833.316	$C_{30}H_{26}O_{12}$	578.1424	$[M-H]^-$	577.1347	Proanthocyanidins
Cosmosiin	163955.198	$C_{21}H_{20}O_{10}$	432.1056	$[M-H]^-$	431.098	Flavones
Calycosin	163702.704	$C_{16}H_{12}O_5$	284.0685	$[M+H]^+$	285.0763	Isoflavones
3′-O-Methyltricetin-7-O-glucoside	160,313	$C_{22}H_{22}O_{12}$	478.1111	$[M+H]^+$	479.119	Flavones

(*continued on next page*)

Table 1 (*continued*)

name	metabolite abundance	Formula	Molecular weight (Da)	Ionization model	Q1 (Da)	Class II
7-hydroxy-3-(2-methoxyphenyl)-4H-chromen-4-one	158899.877	$C_{16}H_{12}O_4$	268.0735589	$[M-H]^-$	267.066	Isoflavones
Kaempferol-3-O-neohesperidoside*	157957.5	$C_{27}H_{30}O_{15}$	594.1585	$[M+H]^+$	595.1636	Flavonols
5,7,3′,4′-Tetrahydroxy-6,8-dimethoxyflavone	146806.09	$C_{17}H_{14}O_8$	346.0688675	$[M-H]^-$	345.0613	Flavones
Epicatechin-4′-O-β-D-glucopyranoside*	140626.183	$C_{21}H_{24}O_{11}$	452.1319	$[M-H]^-$	451.1271	Flavanols
Mearnsetin-3-O-glucoside	138879.864	$C_{22}H_{22}O_{13}$	494.106	$[M-H]^-$	493.0963	Flavones
2-(3,4-dihydroxyphenyl)-4h-chromene-3,5,7-triol-glucoside	137,199	$C_{21}H_{22}O_{11}$	450.1162	$[M+H]^+$	451.1232	Flavanols
Dihydrocharcone-4′-O-glucoside	136175.142	$C_{21}H_{24}O_{10}$	436.1369	$[M-H]^-$	435.1301	Chalcones
Nicotiflorin*	134912.25	$C_{27}H_{30}O_{15}$	594.1585	$[M+H]^+$	595.1622	Flavonols
Procyanidin C2	133610.953	$C_{45}H_{38}O_{18}$	866.2058	$[M-H]^-$	865.2063	Proanthocyanidins
Kaempferol-3-O-glucoside-7-O-rhamnoside*	132801.25	$C_{27}H_{30}O_{15}$	594.1585	$[M+H]^+$	595.1658	Flavonols
Chrysoeriol-6-C-glucoside-4′-O-glucoside	127653.5	$C_{28}H_{32}O_{16}$	624.169	$[M+H]^+$	625.1764	Flavones
Epicatechin glucoside*	125615.677	$C_{21}H_{24}O_{11}$	452.1319	$[M-H]^-$	451.1244	Flavanols
Quercetin-3-O-(6′′-O-galloyl)glucoside	123596.5	$C_{28}H_{24}O_{16}$	616.1064	$[M+H]^+$	617.1132	Flavonols
Naringenin (5,7,4′-Trihydroxyflavanone)	118345.369	$C_{15}H_{12}O_5$	272.0685	$[M-H]^-$	271.0625	Flavanones
Dihydrokaempferol-3-O-glucoside	115,411	$C_{21}H_{22}O_{11}$	450.1162	$[M+H]^+$	451.1211	Flavanonols
saffloquinoside A	111233.972	$C_{27}H_{30}O_{15}$	594.1585	$[M+H]^+$	595.1663	Chalcones
Quercetin-3-O-(2′′-O-galloyl)galactoside	104888.75	$C_{28}H_{24}O_{16}$	616.1064	$[M+H]^+$	617.1181	Flavonols
6-Hydroxyluteolin	103606.898	$C_{15}H_{10}O_7$	302.0427	$[M-H]^-$	301.0351	Flavones
Luteolin-6-C-arabinoside-7-O-glucoside	100,717	$C_{26}H_{28}O_{15}$	580.1428	$[M+H]^+$	581.1526	Flavones
5-hydroxy-7,8,3′,4′-tetramethoxyflavone glucoside	100372.75	$C_{25}H_{28}O_{12}$	520.1581	$[M+H]^+$	521.1636	Flavones
Marein	99,473	$C_{21}H_{22}O_{11}$	450.1162	$[M+H]^+$	451.1243	Chalcones
O-MethylNaringenin-8-C-arabinoside	98706.25	$C_{21}H_{22}O_9$	418.1264	$[M+H]^+$	419.1343	Flavanones
Eriodictyol-3′-O-glucoside	94354.043	$C_{21}H_{22}O_{11}$	450.1162	$[M-H]^-$	449.109	Flavanones
4′-O-Glucosylvitexin	92921.75	$C_{27}H_{30}O_{15}$	594.1585	$[M+H]^+$	595.1671	Flavones
6-Hydroxyluteolin 5-glucoside	92842.759	$C_{21}H_{20}O_{12}$	464.0955	$[M-H]^-$	463.0889	Flavones
Naringenin chalcone; 2′,4,4′,6′-Tetrahydroxychalcone	89625.035	$C_{15}H_{12}O_5$	272.0685	$[M+H]^+$	273.0769	Chalcones
Neohesperidin	88453.066	$C_{28}H_{34}O_{15}$	610.1898	$[M-H]^-$	609.182	Flavanones
Quercetin-3-O-(6′′-O-p-Coumaroyl)glucoside	87003.509	$C_{30}H_{26}O_{14}$	610.1323	$[M+H]^+$	611.1382	Flavonols

*means that the component may have isomers.

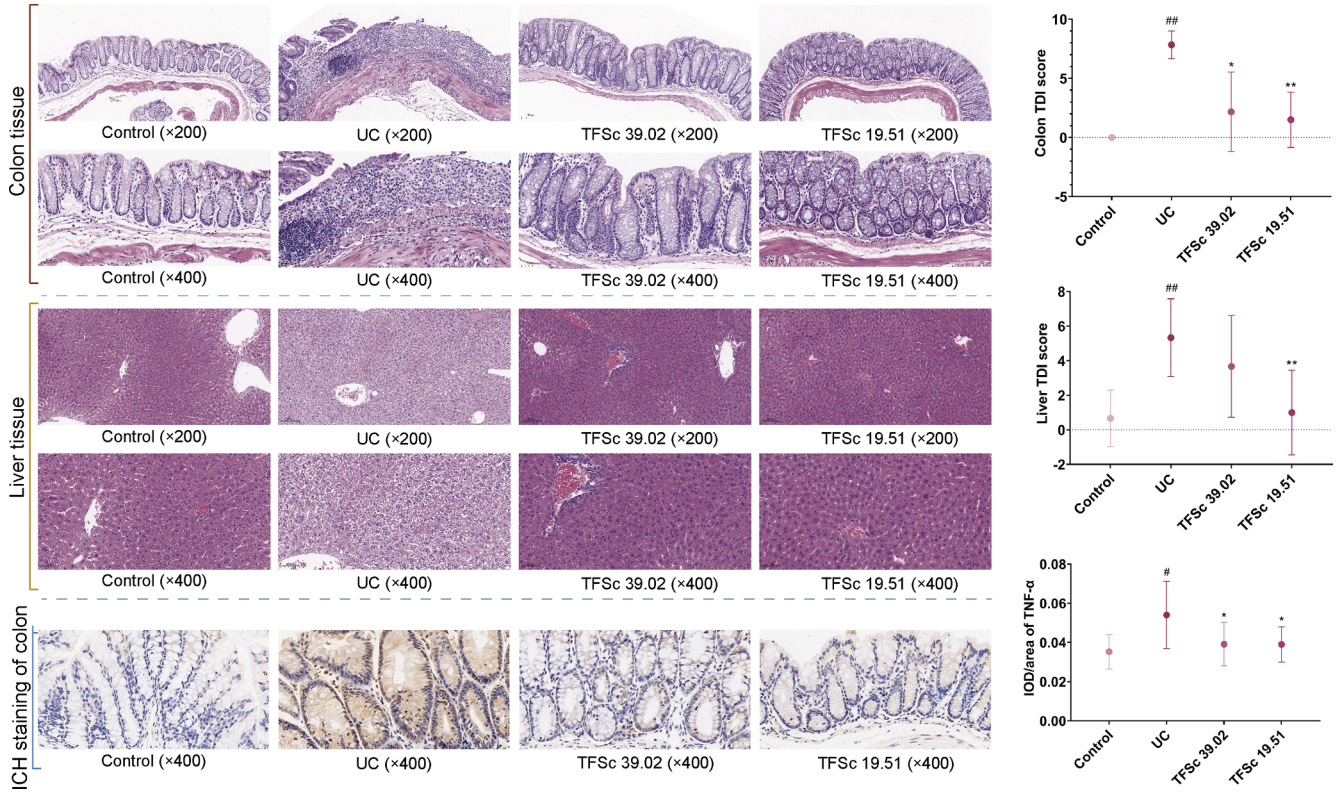

Fig. 3. Representative HE and IHC histological sections, TDI scores of colons and livers (200 × and 400 × magnification), and the integrated optical density (IOD)/area values of TNF-α in the colons (400 × magnification). Data are presented as mean ± SD (n = 6 per group). $^{\#}P < 0.05$ vs. the control group, $^{\#\#}P < 0.01$ vs. the control group, $^{*}P < 0.05$ vs. the UC group, $^{**}P < 0.01$ vs. the UC group.

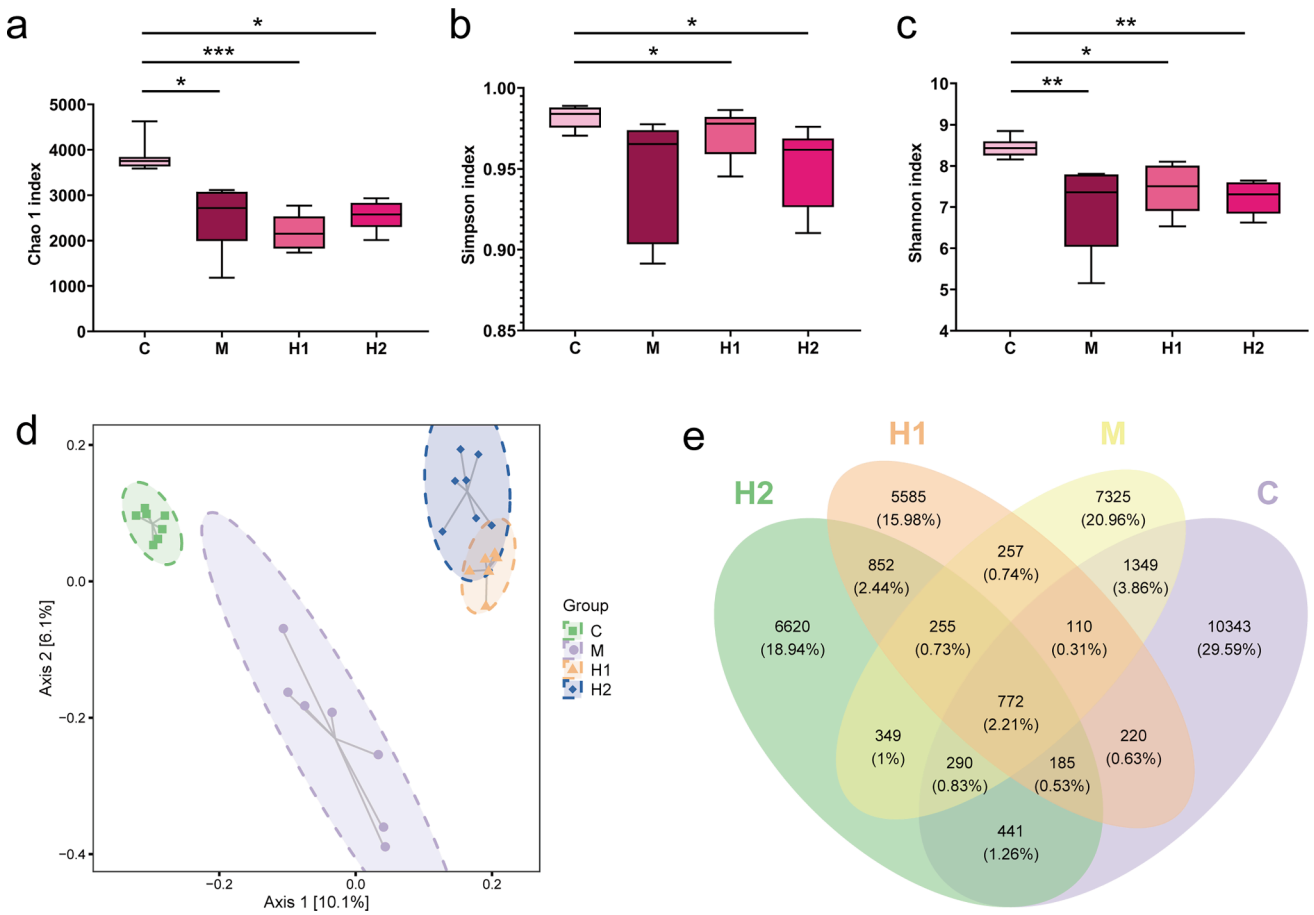

Fig. 4. Total flavonoids of *Sargentodoxa cuneata* (TFSc) affected the intestinal flora in mice with UC. (**a**) chao1 index. (**b**) Simpson index. (**b**) Shannon index. (**d**) PCoA analysis results of control group (C), UC group (M), and high- (H1) and low-dose (H2) TFSc groups. (**e**) The Venn graph. (n = 7 per group). $^{*}P < 0.05$ vs. the control group, $^{**}P < 0.01$ vs. the control group, and $^{***}P < 0.001$ vs. the control group.

kg) reduced colonic tissue damage and inflammatory cell infiltration, as well as the colon TDI score ($P < 0.05$) (Fig. 3). In addition, cellular enlargement, cytoplasmic vacuolation, narrowing of the hepatic sinusoids, and slight inflammatory infiltrates were observed in mice with UC. This is consistent with the literature reporting that UC causes liver damage (Guan et al., 2022). TFSc improved the aforementioned pathological changes and decreased the liver TDI scores. These results indicate that TFSc ameliorated both colon and liver injuries in mice with UC.

3.3. TFSc decreased the levels of TNF-α in the colon tissues in mice with UC

After induction by DSS, the levels of TNF-α in the mouse colon increased significantly ($P \leq 0.05$), indicating the presence of immunoinflammatory injury in the mouse colon tissues. After treatment with TFSc, the levels of TNF-α in the colon of the animals reduced significantly, indicating that TFSc has a favorable anti-inflammatory protective effect on mice with UC (Fig. 3).

3.4. TFSc regulated gut microbiota dysbiosis in mice with UC

16S rRNA gene sequencing demonstrated that DSS treatment reduced the Chao1 (Fig. 4a), Simpson (Fig. 4b), and Shannon (Fig. 4c) indices. The TFSc dose of 39.02 mg/kg increased the Simpson and Shannon indices, suggesting recovery of intestinal microbial richness and diversity. However, the 19.51 mg/kg TFSc dose had less effect on intestinal microbial richness and diversity. Furthermore, PCoA plot of the groups revealed that the control, UC, and TFSc-treated groups were distributed across different spatial regions (Fig. 4d). The Venn graph and number of taxa in the gut microbiota are shown in Fig. 4e. These results suggest that TFSc modulates the diversity and relative abundance of intestinal flora in mice with UC.

The heatmap shows that the flora significantly altered by TFSc intervention primarily included Anaeroplasma, Turicibacter, Parabacteroides, Anaerotruncus, Mucispirillum, Corynebacterium, Odoribacter, Staphylococcus, Akkermansia, Streptococcus, Shigella, Proteus, Prevotella, and Lactobacillus (Fig. 5a). Fig. 5b and c show the bar plots of the gut microbiota at family and genus levels, respectively. TFSc significantly affected abundance of Bacteroides, Shigella, Allobaculum, Lactobacillus, Ruminococcus, Prevotella, and [Prevotella] at the genus level.

Furthermore, LEfSe analysis was used to determine the differential intestinal flora in each group. A total of 81 taxa were identified from phylum to genus, including 25 taxa in the control group, 26 in the UC group, 11 in the high-dose TFSc group, and 19 in the low-dose TFSc group (Fig. 6). Differential flora in the 39.02 mg/kg TFSc group included Dehalobacterium, Peptococcaceae, Epsilonproteobacteria, Helicobacteraceae, Campylobacterales, Faecalibacterium, Rikenellaceae, Ruminococcus, Clostridiales, Clostridia, and Dehalobacteriaceae. Differential flora in the 19.51 mg/kg TFSc group included [Paraprevotellaceae], Alphaproteobacteria, RF32, YS2, 4C0d_2, Erysipelotrichaceae, Clostridium, Peptostreptococcaceae, rc4_4, Desulfovibrio, Sutterella, Alcaligenaceae, Desulfovibrionales, Desulfovibrionaceae, Deltaproteobacteria, Betaproteobacteria, Burkholderiales, RF3, ML615J_28, and [Prevotella] (Fig. 6b).

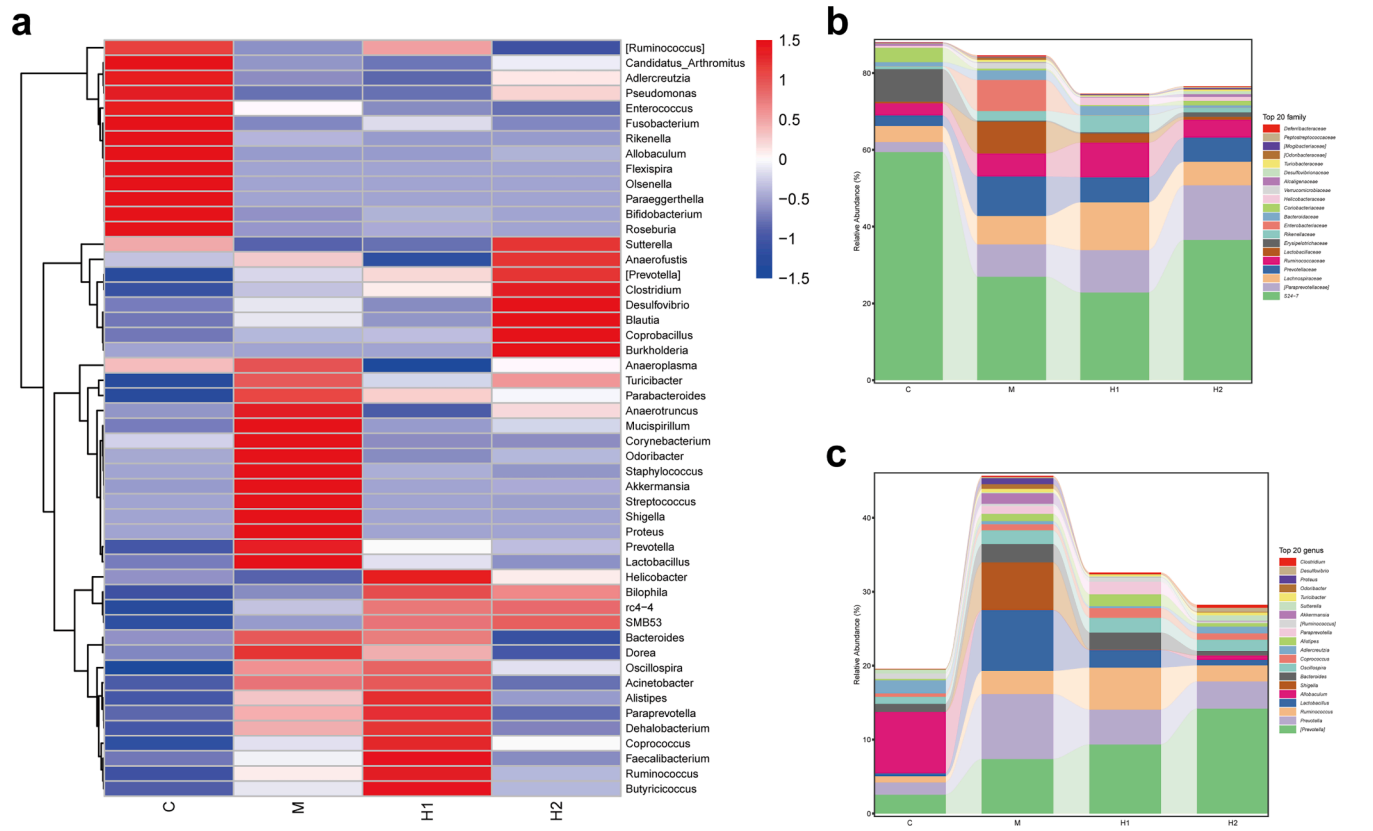

Fig. 5. Total flavonoids of *Sargentodoxa cuneata* (TFSc) affected the relative abundance of intestinal flora in mice with UC. (**a**) The heatmap analysis. (**b**, **c**) The relative abundance of intestinal flora at the family and genus levels. The control group: C, UC group: M, high-dose TFSc group (H1), and low-dose TFSc group (H2) (n = 7 per group).

3.5. TFSc affected the levels of SCFAs and organic acids, and results of Spearman's correlation analysis

Compared to the control group, isobutyric acid, ethylmethylacetic acid, and succinic acid levels were reduced ($P < 0.01$), while malonic acid levels were increased in mice with UC ($P < 0.05$). The 39.02 mg/kg TFSc group demonstrated increased levels of isocaproic acid, 3-hydroxyisovaleric acid, and glutaric acid levels ($P < 0.05$) in the intestines. The 19.51 mg/kg TFSc group exhibited significantly increased levels of isobutyric acid and ethylmethylacetic acid ($P < 0.01$). Further, TFSc (39.02 and 19.51 mg/kg) significantly decreased the levels of malonic acid and succinic acid ($P < 0.05$) in the intestinal contents (Fig. 7).

Moreover, a significant correlation of intestinal flora with differential SCFAs and organic acids was observed in each group at family (Fig. 8a, c, e) and genus levels (Fig. 8b, d, f). Spearman's correlation analysis suggested that malonic acid, valeric acid, ethylmethylacetic acid, and isobutyric acid were associated with different gut flora (Fig. 8a, b). Succinic acid, hexanoic acid, glutaric acid, 3-hydroxyisovaleric acid, and isocaproic acid in high-dose TFSc group were associated with Bifidobacteriaceae, Peptococcaceae, Helicobacteraceae, Corynebacteriaceae, [Odoribacteraceae], Deferribacteraceae, Anaeroplasmataceae, Bifidobacterium, Proteus, Candidatus_Arthromitus, Anaeroplasma, Corynebacterium, Odoribacter, Rikenella, and Mucispirillum (Fig. 8c, d). Differential SCFAs and organic acids in the low-dose TFSc group were also found to be strongly associated with the intestinal flora (Fig. 8e, f).

Comparing the results of high- and low-dose TFSc groups (Fig. 8) demonstrated that TFSc exerts ameliorative effects on colon and liver injuries by modulating Bifidobacteriaceae, Helicobacteraceae, Corynebacteriaceae, [Odoribacteraceae], Bifidobacterium, Proteus, Corynebacterium, Odoribacter, and Rikenella, thereby affecting SCFAs and organic acids.

4. Discussion

UC is a serious threat to human health and is accompanied by economic and psychological burden, which affects their long-term quality of survival (Ghosh et al., 2021). UC also causes liver injury, arthritis, skin and mucous membrane diseases, intestinal perforation, toxic megacolon, intestinal obstruction, colorectal cancer and other complications that pose serious threats to human health (Eder et al., 2023). UC is related to genetics, diet, immuno-inflammation, and intestinal flora; and intestinal flora is an important factor in the development of UC (Huang et al., 2023). Total flavonoids have been proved to be one of the main active components in Chinese herbs used to treat UC (Li et al., 2022a), which guides the direction of identifying the effective site of *Sargentodoxa cuneata* for the treatment of UC. In this study, we found that TFSc significantly ameliorated weight loss, reduced DAI score, improved colon length in mice induced by DSS, and significantly reduced cardiac and hepatic indices, suggesting that TFSc has a favorable protective effect on mice with UC. It can also be deduced that TFSc may be used to provide protection against liver and heart injuries. Furthermore, the results of HE staining showed that TFSc had a good ameliorating effect on both colon and liver injuries in mice with UC. TFSc also decreased the TNF-α levels in colon tissues. Notably, our study found that the gut microbiota is an important pathway through which TFSc improves colon and liver damage in mice with UC. Spearman's correlation analysis revealed that SCFAs and few organic acids may be the direct performers of TFSc in regulating the intestinal flora for treatment of UC.

The human gut is richly colonized by microorganisms that are important for maintaining the integrity of gastrointestinal mucosa, homeostasis of immune system, and regulation of host energy metabolism

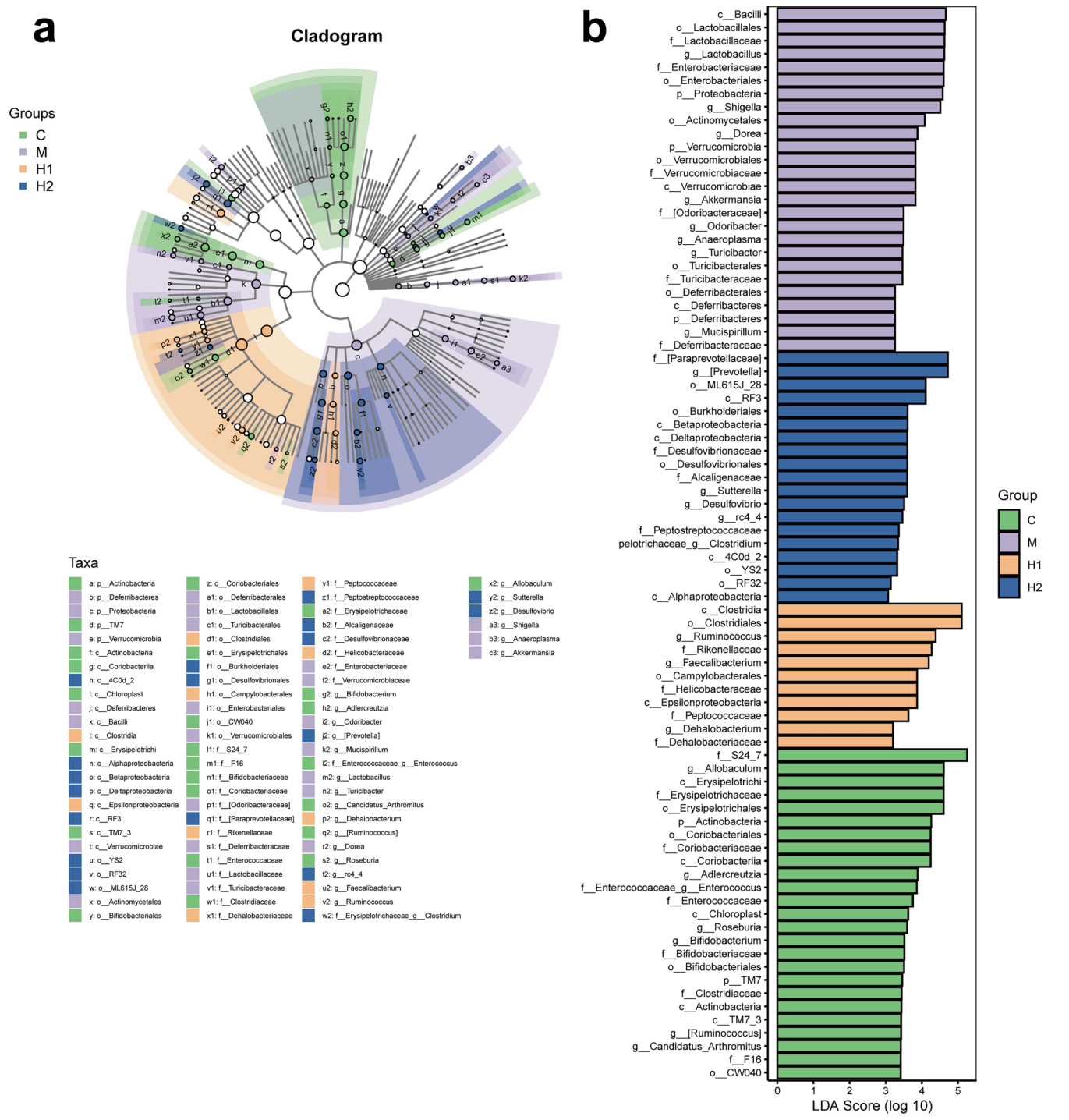

Fig. 6. The results of LEfSe analysis. (**a**) The cladogram results. (**b**) The LDA score (log 10) of each group. The control group: C, UC group: M, high-dose TFSc group (H1), and low-dose TFSc group (H2) (n = 7 per group).

(Lavelle and Sokol, 2020). Clinical disorders of the intestinal flora have been identified in the intestines of patients with UC and are characterized by a reduction in beneficial bacteria and an increase in pathogenic bacteria (Schierová et al., 2020). Mucus and mucin secreted by the intestinal flora together form a mucus layer on the surface of intestinal epithelial cells (Fang et al., 2021). Dysbiosis of the gut microflora can lead to inflammation and abnormal intestinal function, with the intestinal mucosal barrier being the primary challenge (van der Post et al., 2019). A compromised intestinal mucosal barrier will not be able to block the translocation of intestinal parasitic flora and their toxins to tissues and organs outside the intestinal lumen, leading to the exposure of the organism to endogenous microorganisms and their toxins (Philips et al., 2020). Liver, the largest detoxification organ in an organism, is damaged when endotoxin levels are too high (Liu et al., 2020). It has been found that intestinal flora is also closely associated with liver injury, and the gut–liver axis is a crucial pathway for UC treatment (Li et al., 2022b). In the present study, we found that TFSc ameliorated both colon and liver injuries in mice with UC. Moreover, a good protective effect of TFSc on the structural integrity of colonic mucosa was observed in HE staining, suggesting that intestinal flora mediate the amelioration of colon and liver injuries in mice with UC.

Changes in the relative abundance and diversity of the intestinal

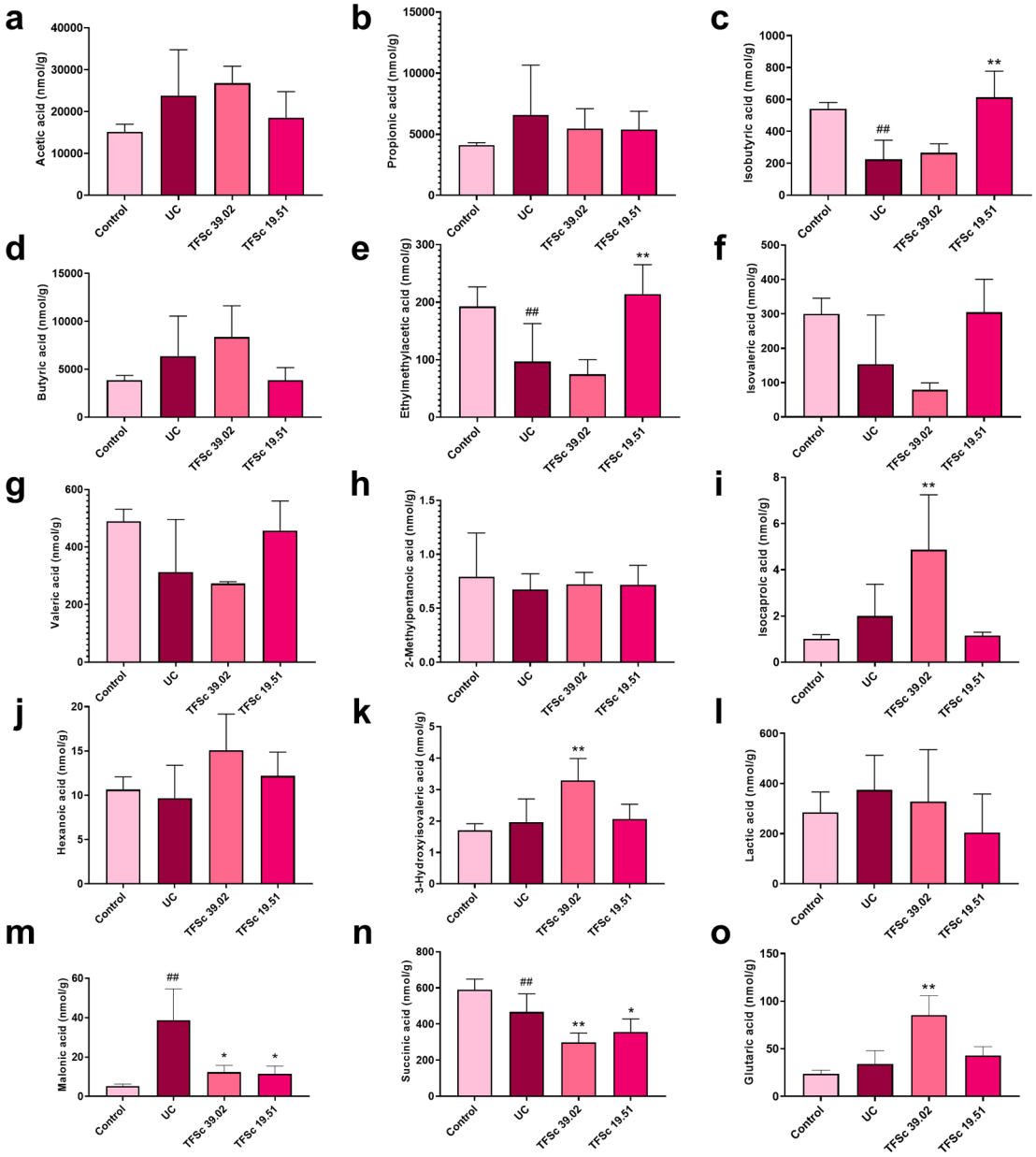

Fig. 7. Total flavonoids of *Sargentodoxa cuneata* (TFSc) affected the levels of SCFAs and few organic acids in the intestinal contents in mice with UC. The data are represented as mean ± SD (n = 6–7 per group). $^{\#}P < 0.05$ vs. the control group, $^{\#\#}P < 0.01$ vs. the control group, $^{*}P < 0.05$ vs. the UC group, $^{**}P < 0.01$ vs. the UC group.

flora can reflect to some extent the effect of drugs on the intestinal flora (Niu et al., 2022). Simpson and Shannon indices, PCoA analysis, Venn graph, heatmap, and relative abundance analysis showed that TFSc had a modulating effect on the intestinal flora of mice with UC. As shown in Fig. 5b, TFSc ameliorated the changes in the relative abundance of S24-7, Prevotellaceae, [Odoribacteraceae], Enterobacteriaceae, Bacteroidaceae, Coriobacteriaceae, Helicobacteraceae, Verrucomicrobiaceae, Turicibacteraceae, and Deferribacteraceae. In addition, TFSc increased the relative abundance of [Paraprevotellaceae], Lachnospiraceae, and Ruminococcaceae.

As shown in Fig. 5c, TFSc ameliorated the changes in the relative abundance of Prevotella, Lactobacillus, Shigella, Bacteroides, Adlercreutzia, [Ruminococcus], Akkermansia, Turicibacter, Odoribacter, and Proteus. Moreover, TFSc increased the relative abundance of [Prevotella], Ruminococcus, Coprococcus, Alistipes, and Clostridium. TFSc increased the relative abundance of beneficial bacteria Coriobacteriaceae (Pittayanon et al., 2020), Adlercreutzia (Galipeau et al., 2021), [Ruminococcus] (Xu et al., 2021), [Prevotella] (Jiang et al., 2023), Coprococcus (Xu et al., 2021), Alistipes (Yuan et al., 2020), and Clostridium (Ma et al., 2022); and decreased the relative abundance of pathogenic bacteria Enterobacteriaceae (Dong et al., 2022), Turicibacteraceae (He et al., 2022), Deferribacteraceae (Yu et al., 2023a), Shigella (Jialing et al., 2020), and Turicibacter (Dong et al., 2022). Lefse analysis is commonly used to identify differential marker flora, which facilitates the understanding of drug modulation in the gut flora (Zhao et al., 2023). After TFSc modulation, mice with UC showed a differential flora of both beneficial and pathogenic bacteria, suggesting that these may be the primary intestinal flora of TFSc against UC, which could be the focus of future in-depth studies.

Both SCFAs and organic acids are metabolites of the intestinal flora. Among these, SCFAs are valuable for maintaining the intestinal immune microenvironment and mucosal barrier (Kaczmarczyk et al., 2021, Kotla and Rochev, 2023). Modern research has shown that high levels of SCFAs have a positive effect on the treatment of UC (Li et al., 2022c).

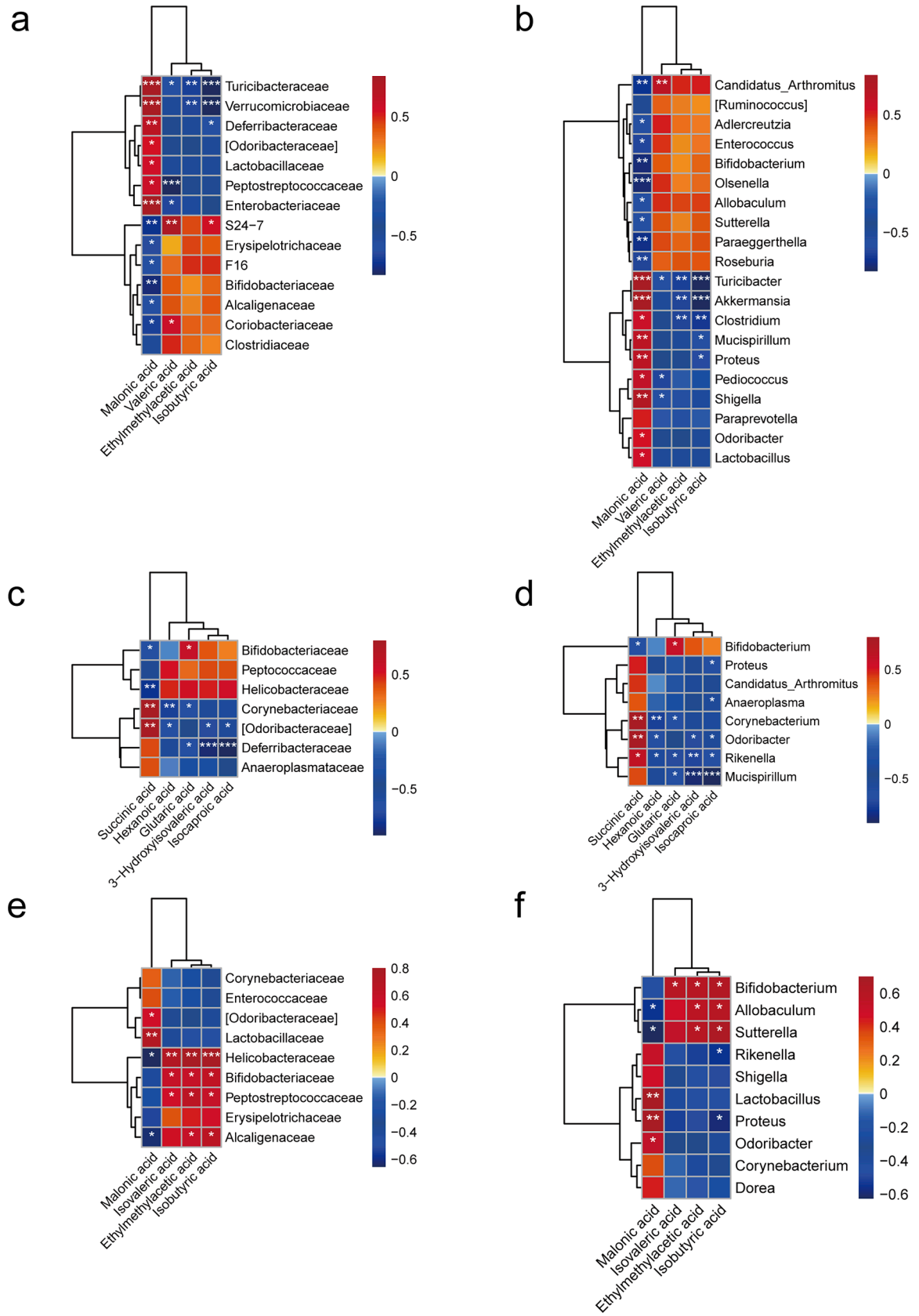

Fig. 8. Correlation analysis results. (**a, b**) The correlation analysis between the intestinal flora and SCFAs and few organic acids levels in the UC group at the family and genus levels. (**c, d**) The correlation analysis between the intestinal flora and SCFAs and few organic acids levels in the high-dose TFSc group at the family and genus levels. (**e, f**) The correlation analysis between the intestinal flora and SCFAs and few organic acids levels in the low-dose TFSc group at the family and genus levels. Significant differences were indicated at $^{*}P < 0.05$, $^{**}P < 0.01$ and $^{***}P < 0.001$.

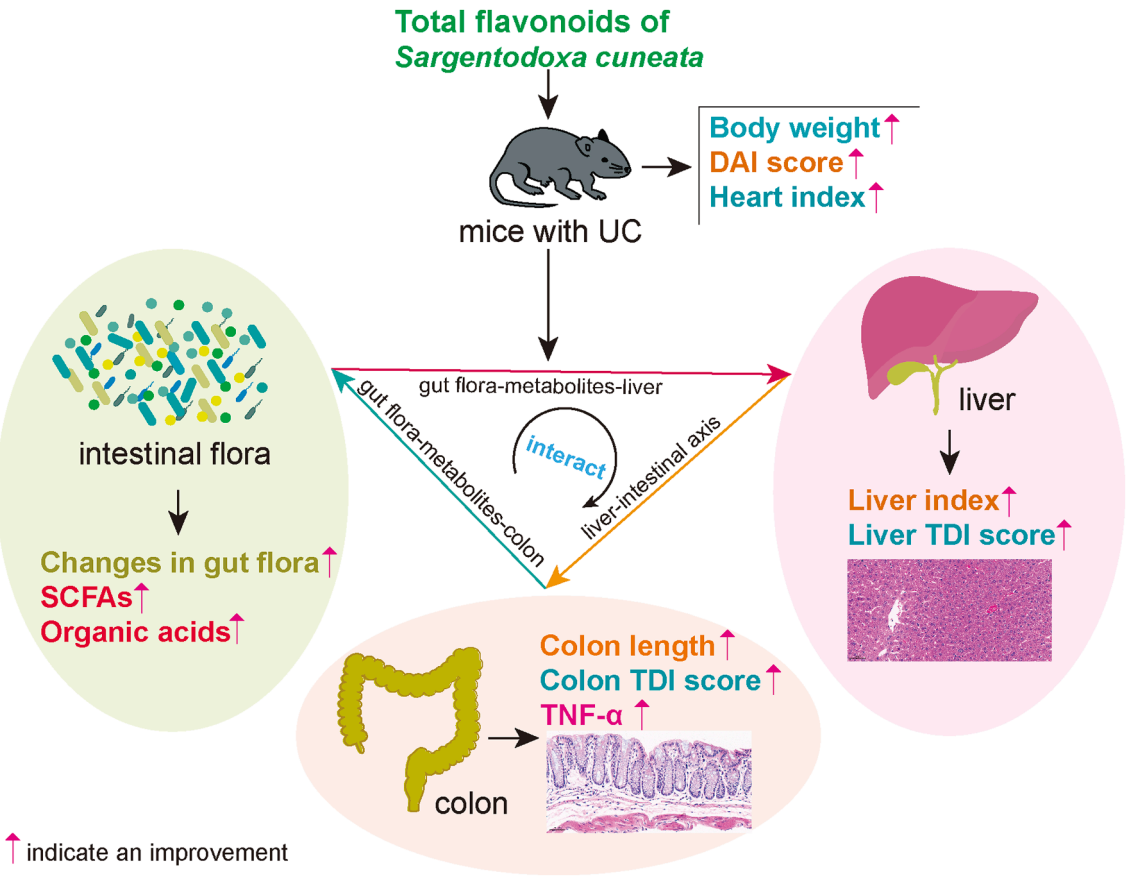

Fig. 9. The potential mechanisms of total flavonoids of *Sargentodoxa cuneata* (TFSc) against UC.

Organic acids in the intestinal microenvironment of healthy humans are also maintained in a relatively stable range, and an excess of harmful organic acids can take their toll on the intestine (Cao et al., 2022). We found a significant decrease in the levels of isobutyric acid, ethylmethylacetic acid, and succinic acid, which is consistent with previous reports (Zhang et al., 2022). However, there was a significant increase in malonic acid levels. Notably, TFSc corrected these changes in the intestinal contents. Furthermore, high-dose (39.02 mg/kg) TFSc increased the levels of 3-hydroxyisovaleric acid and glutaric acid. Glutamic acid can be metabolized from amino acids such as lysine and tryptophan (Bernstein et al., 2020). This suggests that TFSc plays a regulatory role in amino acid metabolism.

Interestingly, using a correlation analysis, we identified the intestinal flora associated with differential SCFAs and organic acids. Bifidobacteriaceae, Helicobacteraceae, Corynebacteriaceae, [Odoribacteraceae], Bifidobacterium, Proteus, Corynebacterium, Odoribacter, and Rikenella were the same groups of bacteria associated with differential SCFAs or organic acids in the high- and low-dose TFSc groups. Bifidobacteriaceae have been reported as SCFA-producing intestinal flora (Lee et al., 2020), However, whether other analyzed flora are SCFA-producing has not been reported in the literature, and further studies are needed.

Our study had a few limitations that need consideration. First, the effect of TFSc on the intestinal mucosal barrier was illustrated only by HE-stained sections and no directly related proteins were tested for validation. Second, the effect of TFSc on the intestinal flora of mice with UC was studied only up to the genus level and not specifically which bacteria were altered, which can be addressed in later studies. Finally, no evidence was provided regarding whether TFSc affected other metabolites in the gut flora and further studies are needed.

5. Conclusion

TFSc has a beneficial effect on colon and liver injuries in mice with UC. Its associated pharmacological mechanism of action may be related to correcting intestinal flora disorders, elevating the levels of SCFAs (isocaproic acid, 3-hydroxyisovaleric acid, isobutyric acid, and ethylmethylacetic acid), lowering the levels of organic acids (malonic acid and succinic acid), and protecting the integrity of the intestinal mucosa. TFSc may affect SCFAs and organic acid levels by regulating Bifidobacteriaceae, Helicobacteraceae, Corynebacteriaceae, [Odoribacteraceae], Bifidobacterium, Proteus, Corynebacterium, Odoribacter, and Rikenella, which in turn protects the intestinal mucosal barrier (Fig. 9).

CRediT authorship contribution statement

Feng Xu: Writing – original draft, Funding acquisition, Validation, Investigation, Methodology, Supervision, Conceptualization, Writing – review & editing. **Piao Yu:** Investigation. **Hongmei Wu:** Methodology, Supervision. **Xiangpei Wang:** Methodology, Supervision. **Mei Liu:** Investigation. **Hongyun Liu:** Investigation. **Qian Zeng:** Investigation. **Dengli Wu:** Investigation.

Declaration of competing interest

The authors declare that they have no known competing financial interests or personal relationships that could have appeared to influence the work reported in this paper.

Acknowledgments

We would like to thank grants from Guizhou Provincial Basic Research Program (Natural Science) (Qian Kehe Foundation ZK [2022] General 497), Guizhou University of Traditional Chinese Medicine 2021 National Natural Science Foundation of China Post-subsidy Fund Scientific Research Innovation Exploration Special Project (2018YFC170810-505), and the Scholarship Fund from the China Scholarship Council (No. 202208520056).

Appendix A. Supplementary data

Supplementary data to this article can be found online at https://doi.org/10.1016/j.arabjc.2023.105566.

References

Bernstein, L., Coughlin, C.R., Drumm, M., et al., 2020. Inconsistencies in the nutrition management of glutaric aciduria type 1: An international survey. Nutrients 12, 3162.
Cao, C., Wang, L., Ai, C., et al., 2022. Impact of Lycium barbarum arabinogalactan on the fecal metabolome in a DSS-induced chronic colitis mouse model. Food Funct. 13, 8703–8716.
Chen, Y., Wang, P., Zhang, Y., et al., 2022. Comparison of effects of aminosalicylic acid, glucocorticoids and immunosuppressive agents on the expression of multidrug-resistant genes in ulcerative colitis. Sci. Rep. 12, 20656.
Cheng, H., Liu, J., Zhang, D., et al., 2022. Gut microbiota, bile acids, and nature compounds. Phytother. Res. 36, 3102–3119.
Cheng, H., Zhang, D., Wu, J., et al., 2023. Interactions between gut microbiota and polyphenols: A mechanistic and metabolomic review. Phytomedicine 154979.
Cleveland, N.K., Torres, J., Rubin, D.T., 2022. What does disease progression look like in ulcerative colitis, and how might it be prevented? Gastroenterology 162, 1396–1408.
Dong, L., Du, H., Zhang, M., et al., 2022. Anti-inflammatory effect of Rhein on ulcerative colitis via inhibiting PI3K/Akt/mTOR signaling pathway and regulating gut microbiota. Phytother. Res. 36, 2081–2094.
Eder, P., Łodyga, M., Gawron-Kiszka, M., et al., 2023. Guidelines for the management of ulcerative colitis. Recommendations of the Polish Society of Gastroenterology and the Polish National Consultant in Gastroenterology. Gastroenterol. Rev./przegląd Gastroenterologiczny 18.
Fang, J., Wang, H., Zhou, Y., et al., 2021. Slimy partners: The mucus barrier and gut microbiome in ulcerative colitis. Exp. Mol. Med. 53, 772–787.
Galipeau, H.J., Caminero, A., Turpin, W., et al., 2021. Novel fecal biomarkers that precede clinical diagnosis of ulcerative colitis. Gastroenterology 160, 1532–1545.
Ghosh, S., Sanchez Gonzalez, Y., Zhou, W., et al., 2021. Upadacitinib treatment improves symptoms of bowel urgency and abdominal pain, and correlates with quality of life improvements in patients with moderate to severe ulcerative colitis. J. Crohns Colitis 15, 2022–2030.
Guan, F., Luo, H., Wu, J., et al., 2022. Andrographolide sodium bisulfite ameliorates dextran sulfate sodium-induced colitis and liver injury in mice via inhibiting macrophage proinflammatory polarization from the gut-liver axis. Int Immunopharmacol 110, 109007.
He, Y., Luo, R., Xia, M., et al., 2022. Orally administered diosgenin alleviates colitis in mice induced by dextran sulfate sodium through gut microbiota modulation and short-chain fatty acid generation. J. Med. Food 25, 261–271.
Huang, C., Hao, W., Wang, X., et al., 2023. Probiotics for the treatment of ulcerative colitis: a review of experimental research from 2018 to 2022. Front. Microbiol. 14.
Jialing, L., Yangyang, G., Jing, Z., et al., 2020. Changes in serum inflammatory cytokine levels and intestinal flora in a self-healing dextran sodium sulfate-induced ulcerative colitis murine model. Life Sci. 263, 118587.
Jiang, K., Wang, D., Su, L., et al., 2023. Tamarind seed polysaccharide hydrolysate ameliorates dextran sulfate sodium-induced ulcerative colitis via regulating the gut microbiota. Pharmaceuticals 16, 1133.
Kaczmarczyk, O., Dąbek-Drobny, A., Woźniakiewicz, M., et al., 2021. Fecal levels of lactic, succinic and short-chain fatty acids in patients with ulcerative colitis and crohn disease: A pilot study. J. Clin. Med. 10, 4701.
Kotla, N.G., Rochev, Y., 2023. IBD disease-modifying therapies: insights from emerging therapeutics. Trends Mol. Med.
Lai, S., 2019. Study on the chemical constituents of Sargentodoxa cuneata and Helvella leucopus 硕士, Shanxi Normal Universty.
Lavelle, A., Sokol, H., 2020. Gut microbiota-derived metabolites as key actors in inflammatory bowel disease. Nat. Rev. Gastroenterol. Hepatol. 17, 223–237.
Le Berre, C., Honap, S., Peyrin-Biroulet, L., 2023. Ulcerative colitis. Lancet 402, 571–584. https://doi.org/10.1016/S0140-6736(23)00966-2.
Lee, J., d'Aigle, J., Atadja, L., et al., 2020. Gut microbiota–derived short-chain fatty acids promote poststroke recovery in aged mice. Circ. Res. 127, 453–465.
Li, P., Chen, G., Zhang, J., et al., 2022c. Live Lactobacillus acidophilus alleviates ulcerative colitis via the SCFAs/mitophagy/NLRP3 inflammasome axis. Food Funct. 13, 2985–2997.
Li, C., Wang, L., Zhao, J., et al., 2022a. Lonicera rupicola Hook. f. et Thoms flavonoids ameliorated dysregulated inflammatory responses, intestinal barrier, and gut microbiome in ulcerative colitis via PI3K/AKT pathway. Phytomedicine 104, 154284.
Li, L., Wang, Y., Zhao, L., et al., 2022b. Sanhuang xiexin decoction ameliorates secondary liver injury in DSS-induced colitis involve regulating inflammation and bile acid metabolism. J. Ethnopharmacol. 299, 115682.
Liu, Y., Wu, J., Chen, L., et al., 2020. β-patchoulene simultaneously ameliorated dextran sulfate sodium-induced colitis and secondary liver injury in mice via suppressing colonic leakage and flora imbalance. Biochem. Pharmacol. 182, 114260.
Liu, Y., Li, B.-G., Su, Y.-H., et al., 2022. Potential activity of traditional Chinese medicine against ulcerative colitis: a review. J. Ethnopharmacol. 289, 115084.
Ma, L., Shen, Q., Lyu, W., et al., 2022. Clostridium butyricum and its derived extracellular vesicles modulate gut homeostasis and ameliorate acute experimental colitis. Microbiol. Spectrum 10, e01368.
Niu, W., Chen, Y., Wang, L., et al., 2022. The combination of sodium alginate and chlorogenic acid enhances the therapeutic effect on ulcerative colitis by the regulation of inflammation and the intestinal flora. Food Funct. 13, 10710–10723.
Philips, C.A., Augustine, P., Yerol, P.K., et al., 2020. Modulating the intestinal microbiota: therapeutic opportunities in liver disease. J. Clin. Transl. Hepatol. 8, 87.
Pittayanon, R., Lau, J.T., Leontiadis, G.I., et al., 2020. Differences in gut microbiota in patients with vs without inflammatory bowel diseases: a systematic review. Gastroenterology 158 (930–946), e931.
Schierová, D., Březina, J., Mrázek, J., et al., 2020. Gut microbiome changes in patients with active left-sided ulcerative colitis after fecal microbiome transplantation and topical 5-aminosalicylic acid therapy. Cells 9, 2283.
Upadhyay, K.G., Desai, D.C., Ashavaid, T.F., et al., 2023. Microbiome and metabolome in inflammatory bowel disease. J. Gastroenterol. Hepatol. 38, 34–43. https://doi.org/10.1111/jgh.16043.
van der Post, S., Jabbar, K.S., Birchenough, G., et al., 2019. Structural weakening of the colonic mucus barrier is an early event in ulcerative colitis pathogenesis. Gut 68, 2142–2151.
Wang, M., Fu, R., Xu, D., et al., 2023a. Traditional Chinese Medicine: a promising strategy to regulate the imbalance of bacterial flora, impaired intestinal barrier and immune function attributed to ulcerative colitis through intestinal microecology. J. Ethnopharmacol. 318, 116879 https://doi.org/10.1016/j.jep.2023.116879.
Wang, Y., Zhang, B., Liu, S., et al., 2023b. The traditional herb Sargentodoxa cuneata alleviates DSS-induced colitis by attenuating epithelial barrier damage via blocking necroptotic signaling. J. Ethnopharmacol. 117373.
Xu, N., Bai, X., Cao, X., et al., 2021. Changes in intestinal microbiota and correlation with TLRs in ulcerative colitis in the coastal area of northern China. Microb. Pathog. 150, 104707.
Xue, J.C., Yuan, S., Meng, H., et al., 2023. The role and mechanism of flavonoid herbal natural products in ulcerative colitis. Biomed Pharmacother 158, 114086. https://doi.org/10.1016/j.biopha.2022.114086.
Yu, D., Dai, Q., Wang, Z., et al., 2023a. ARF1 maintains intestinal homeostasis by modulating gut microbiota and stem cell function. Life Sci. 328, 121902.
Yu, P., Xu, F., Wu, H., et al., 2023b. Anti-Ulcerative Colitis Effects and Active Ingredients in Ethyl Acetate Extract from Decoction of Sargentodoxa cuneata. Molecules 28, 7663.
Yuan, Z., Yang, L., Zhang, X., et al., 2020. Therapeutic effect of n-butanol fraction of Huang-lian-Jie-du Decoction on ulcerative colitis and its regulation on intestinal flora in colitis mice. Biomed. Pharmacother. 121, 109638.
Zhan, X., Pei, J., Fan, W., et al., 2022. Chemical constituents from ethyl acetate extract of Sargentodoxa cuneata rattans. J Chinese Med. Mater. 45, 1114–1118.
Zhang, W., Sun, C., Zhou, S., et al., 2021. Recent advances in chemistry and bioactivity of Sargentodoxa cuneata. J. Ethnopharmacol. 270, 113840.
Zhang, Z., Zhang, H., Chen, T., et al., 2022. Regulatory role of short-chain fatty acids in inflammatory bowel disease. Cell Commun. Signal. 20, 1–10.
Zhao, H., Ding, T., Chen, Y., et al., 2023. Arecoline aggravates acute ulcerative colitis in mice by affecting intestinal microbiota and serum metabolites. Front. Immunol. 14.